Journal of Al-Azhar University Engineering Sector

Vol. 17, No. 64, July 2022, 974 - 991

ABSORPTION AIR CONDITIONING SYSTEM USING SEAWATER FOR AIR PRECOOLING

H.A. Etaiwe[1], R.Y. Sakr[1], M. R. Salem[1], H.E. Abdelrahman[1]

[1]Mechanical Engineering Department ،Faculty of Engineering at Shoubra, Benha University, Cairo, Egypt

*Corresponding author's E-mail: Husain965@yahoo.com

Received: 23 March 2022 Accepted: 3 April 2022

Abstract:

Cold seawater is an important renewable energy source that can be used in the field of air conditioning. In the northern Arabian Gulf, the depth of seawater ranges from 40 m to 60 m, with seawater temperatures ranging from 15°C to 27°C, which is insufficient for use as a direct seawater method for air conditioning in high-temperature conditions. In this paper, two single effect LiBr-H_2O absorption air conditioning systems that utilize seawater are studied. The seawater is used in the first system for cooling the cooling water required for both the condenser and the absorber. While the second system utilizes seawater for cooling, cooling water is required for the condenser and absorber as well as the air precooling process. The generator temperature varied from 90^{o}C to 110^{o}C. Completer thermodynamics analysis is performed using EES software and the results show that the coefficient of performance for two systems is the same while a considerable reduction of the equipment size is prevailed due to air precooling.

Keywords*:* absorption system, seawater cooling, air pre-cooling, heat exchanger.

استخدام ماء البحر لتبريد الهواء الابتدائي لمنظومة تكييف الهواء الماصه

حسين علي عتيوي[1], رمضان يوسف صقر[1],محمد رضا سالم[1] ,هاني عبد الرحمن الصاوي

قسم الهندسه الميكانيكيه, كلية هندسة شبرا, جامعة بنها, القاهره , مصر

* البريد الإلكتروني للمؤلف الرئيسي : Husain965@yahoo.com

الملخص

ماء البحر يعتبر مصدر مهم لاستخدامه كطاقه نظيفة في حقل تكييف الهواء. تتراوح الأعماق في شمال الخليج العربي بين ٤٠ م الى ٦٠ م بدرجة حراره تتراوح بين ١٥ م الى ٢٧ م وهي غير كافيه لاستخدامها بطرية التبريد المباشر لتكييف الهواء ز في هذه الورقة استخدام منظومتان لبروميد الليثيوم – ماء الماصه مع ماء البحر, المنظومه الأولى استخدام ماء البحر لتبريد المكثف والماص بينما المنظومه الثانيه فيها استخدام ماء البحر لتبيريد الماص مع المكثف إضافة الى استخدام ماء البحر لتبريد الهواء الابتدائي ز. درجة حرارة المولد تتراوح بين ٩٠ م الى ١١٠ م . استخدام برنامج حل المعادلات الهندسي (EES) في التحليل الحراري حيث أظهرت النتائج ان أداء المنظومتين يحمل نفس القيمه, الفرق ان حجم المنظومه التي تستخدم ماء البحر لتبريد الهواء الابتدائي تكون اقل حجما.

Nomenclature:

B_i	wet bulb temperature (^oC)	Q_g	generator heat capacity (kW)
cp_a	specific heat of air	Q_{shx}	solution heat exchanger
c_w	cooling freshwater	Q_{pre}	precooling load (kW)
$c_{s.w}$	seawater cooling	R_i	relative humidity
cp_w	water specific heat	t	temperature (^oC)
h	Enthalpy (J/kg)	UA	number of transfer units, kW/^oC
m	solution mass flow rate	V_i	specific volume (m^3/kg)
m_a	air mass(kg)	W_i	specific humidity of the air
P	pressure (kpa)	x	mass fraction of the lithium-bromide
Q_{abs}	absorption load	LMTD	Logarithmic mean temperature difference (^oC)
Q_{cc}	coil cooling load (kW)	COP	Coefficient of performance
Q_c	condenser heat rejected (kW)		
Q_e	evaporator cooling load(kW)		

:

1. INTRODUCTION

As a result of the annual population growth, the global crisis in the history of the energy system, human great consumption requirements, and the high cost of fossil fuel which supplied 80% of electricity global demand [1]. Figure 1 shows the actual and predicted consumption of different fuel types worldwide up to 2020 [2], the global great energy consumption due to air-conditioning the worldwide for household about 40% which contribute 30% of greenhouse emission [3], and as a result of the greenhouse gases emissions that have an impact on the stratospheric ozone depletion. The refrigeration absorption systems have been studied and analyzing by the authors along the years. By considering the steady state, they have studied the pair $LiBr/H_2O$ [٤–٩]. Likewise, for the absorption system, there are multi techniques and methods have been developed to validated the numerical models [١٠ – ١٢]. Ochoa et al., [13] predicted the dynamic analysis and developed a mathematical model of absorption chiller that worked as a single-effect, lithium bromide–water. This model showed good results because of the ability to simulate the behavior of state parameters

such as temperature, concentrations, and pressures when these are subjected to disruptions in the power supply and thermal load. Ochoa et al., [14] investigated the transient performance of a single effect absorption chiller using the pair LiBr/H_2O when the overall heat transfer coefficients are varied in time by updating the thermo-physical properties and convective coefficients. They achieved good results with accepted errors when compared to the manufacturer data, so the model allowed the real behavior of the absorption chiller to be simulated. Lee et al., [15] with several sources of heat, they discussed the optimizing of the generators for H_2O/LiBr for absorption chiller with multi-heat sources, including high/low-temperature generators and waste heat recovery generators. Verification with experimental results was done. They compared the optimized generators with the baseline point and achieved decreasing in the total volume by 59.06% and increasing in the total generation rate by 31.46%. Zaho et al., [16] applied the heat current method for modeling and optimization of a single effect lithium bromide absorption chiller. They concluded that if the generator temperature increases caused an increase in the maximum cooling capacity by a small percent while the increase of the cooling water temperature leads to a significant decrease of the maximum cooling capacity. Also, their results showed a small difference in concentration has a slight effect on the optimal cooling capacity and mainly affects the component design.

Seawater is a main renewable energy source that can be used for air conditioning by two methods [17], the first one is the direct use of seawater to cool down the freshwater heat exchanger, to supply and circulate it through the building [18]. Second, due to a lack of sea depth, it is possible to use seawater as an auxiliary chiller for air conditioning, particularly in seas or lakes with inadequate depth to meet the requirements for cold-water temperature [19]. The northern part of the Arabian Gulf, where the depth ranges from 40 m to 60 m [20], with seawater temperature ranges from 15°C to 27°C, can be used with an auxiliary chiller to cool down freshwater or air.

In this paper, the aim is to investigate the cooling of single effect LiBr–H_2O absorption air conditioning systems using seawater by two options, the first one is to cool the absorber and condenser, and the second is to cool the absorber and condenser as well as precools the mixture of returned air from conditioned space and fresh air.

2 SYSTEM DESCRIPTION AND MODELLING

2.1 System Description

A single effect air conditioning LiBr-H_2O absorption system that utilizes the seawater for cooling the cooling water required for both the absorber and the condenser is illustrated in Fig. 2. The single effect LiBr-H_2O consists of an evaporator, absorber, solution pump, solution heat exchanger, generator, condenser, and expansion valve. The evaporator is kept working at a temperature of 5^{o}C while the generator temperature was varied to take values of 90, 100, and 110^{o}C. Also, the inlet chilled water temperature to the absorption chiller varied from 10 to 14^{o}C. The seawater temperature was varied to have values of 15, 18, 21, 24, and 27^{o}C respectively. The seawater is drawn and pumped, passed through purification filters then to

a heat exchanger where it cools the cooling water required for condenser and absorber cooling. The second absorption system investigated in the current work is depicted in Fig. 3. The only difference between the two systems is that the pumped seawater is divided into two streams; the first stream goes to the precooler placed in the air-handling unit and the other stream goes to the heat exchanger.

2.2 Precooling Process:

Figure 3 shows the absorption system with the air precooling process, the returned air from conditioned space at state point (19) is mixed with fresh air at state point (20) and cooled by a seawater heat exchanger (precooler) from state at point (2١) to a state point (29). Then the air is passed through the cooling coil where it is cooled and dehumidified to state point (22). After the cooling coil, an air intake fan is installed to draw the air and then supply it to the building. The heat exchanger material used for the cooling coil is made from copper metal because it uses fresh water for cooling and it is cheaper than the heat exchanger used for the air precooling process, which is made from aluminum-titanium alloy to resist corrosion caused by seawater. By using ASHRAE Psychometric chart analysis CD, Fig. (4) Shows the psychometric processes.

3 Modeling for Absorption System

The modeling of the described chiller in the previous section aims to evaluate the chiller's performance under various operating conditions. Some assumptions were taken into consideration in order to simplify the model and also to get an accurate approximation of chiller performance. The mathematical model for the absorption system in the research is solved using Engineering Equation Solver (EES) software. This software solves thousands of coupled nonlinear algebraic equations and differential equations with the benefit of the a lot of fluids have thermodynamic property functions built-in. The used assumptions can be summarized as follows:

- Steady operating conditions.
- There is two-pressure level for the used single effect model, the high-pressure level which is the pressure of the generator and condenser, the low-pressure level, which is the pressure of the absorber and evaporator.
- The pressure losses due to the flow in the piping system are negligible.
- There are no heat losses through the components of the chiller
- For the phase change equipment, the minimum heat capacity is considered for the non-phase change stream.

3.1 Mass balance

the mass balance for the chiller and all fluids involved (i.e. refrigerant, water vapor, and LiBr solution) expressed as:

$$\sum_{in} \dot{m} = \sum_{out} \dot{m} \quad (1)$$

Where: $\dot{m}$ is the mass flow rate of the fluid. In addition, salt balance is involving LiBr solution expressed as:

$$\sum_{in} \dot{m} . x = \sum_{out} \dot{m} . x \quad (2)$$

Where: *x* is the concentration percent of LiBr.

3. 2 Energy balance

Applying the 1st law of thermodynamics on the chiller for each component including all pumps and throttling devices expressed as:

$$\dot{Q} - \dot{W} = \sum m . h \quad (3)$$

Where: $\dot{Q}$ is heat transfer rate.

$\dot{W}$ is the work done by the system

h is the enthalpy of the stream.

3.3 Heat Transfer

Except for solution heat exchangers, all of the equipment is in an absorption chiller, Even though both heat and mass transfer happened it is considered as a heat transfer only. The product of the heat transfer area, and the overall heat transfer coefficient, U, is a better way to put the size and performance of heat exchangers in a single parameter (UA value) expressed in the form: $Q = U\ A\ \Delta T_{lm}$ (4)

Where: ΔT_{lm} is the logarithmic mean temperature difference expressed as:

$$\Delta T_{lm} = \frac{\Delta T_1 - \Delta T_2}{\ln \Delta T_1 / \Delta T_2} \quad (5)$$

Where $\Delta T_1, and\ \Delta T_2$ are the temperature differences between the hot and cold fluid depending on the heat exchanger type. In the present work, the cross-flow types have been assumed.

It could be specified the heat exchangers performance by the effectiveness, which is expressed as:

$$\varepsilon = \frac{Q_{act}}{Q_{max}} \quad (6)$$

Where: $Q_{max} = (m. cp)_{min} \quad \Delta T_{max}$

$\Delta T_{max} = T_{h,i} - T_{c,o}$

$T_{h,i}$ = Inlet hot fluid temperature.

$T_{c,o}$ = Outlet cold fluid temperature.

3.4 Precooling balance

$m_a + m_r = m_x = m_s$ (7)

Where

m_a: mass of fresh air
m_r: mass of return air room
m_x: mixing air after cooling seawater
m_s: supply air mass
Qcc= Qe
The mass recirculation ratio for the air used in the present study is 0.8
The heat load of the precooler is given by:

$Q_{precooler} = m_s . Cp_a . \Delta T$

The cooling coil load is given by:

$Q_{cc} = Q\_{room} + Q\_{fresh} - Q_{precooler}$ (8)

4 Results and Discussion:

To check the validity and consistency of the present model, a comparison is made between its results and that obtained by Florides et al., [21] for the given input data illustrated in Table (1) and the maximum percentage deviation between the present result and that of Florides et al., [21] within ±2%.

Table (1) Design parameters for the single effect LiBr-water absorption cooler, Florides et al., [14]

Parameter	Example-value
Evaporator capacity, kW	10
Evaporator temperature, °C	6
Generator solution exit temperature, °C	90
Weak solution mass fraction,	55% LiBr
Strong solution mass fraction	60% LiBr
Solution heat exchanger exit temperature, °C	65
Generator vapor exit temperature, °C	85

Table (2) Comparison between the present result and that of Florides et al., [14]

Item	Present Work	Florides et al. [14]	Difference %
Evaporator capacity, kW	10	10	-
Absorber heat rejected, kW	13.7	13.42	2.09%
Condenser heat rejected, kW	10.6	10.78	-1.67%
Generator heat input, kW	14.3	14.2	0.70%
COP	0.699	0.704	-0.71%

EES is a program used for analyzing and designing absorption systems and is used to evaluate the performance of the system. The thermodynamic properties of lithium bromide–water solution, refrigerant (pure water) as well as humid air were obtained or calculated using the balancing of heat and mass and the equations of heat transfer, the ambient environments, cooling, heat exchanger effectiveness, water inlet temperature, and mass flow rate are among the initial conditions employed by the program. The estimated values of pressure, temperature, enthalpy, mass flow rate, and concentrations for both systems at all points of the cycles by input parameters related to the cooling temperature of seawater to check the performance analysis. Figures 2 and 3 illustrate the state points of the cycle, Tables 1 and 2 show the values of different variables at the points given in both systems illustrated in Figs. 2 and 3 respectively for the conditioned space load is 2000 kW.

Table 1: Values of different variables at different state points for the system given in Fig. 2

Point	T_i	Xi	hi	Bi	p_i	Ri	W_i	Q_i	c_i	v_i	m_i
1	34.46	0.55	83.21		0.8725					1.017	16.95
2		0.55	83.21		9.169						
3	79.2	0.55	175.5		9.169						16.95
4	90	0.6	214.1		9.169				1.957		15.54
5		0.6	113.4		9.169						
6	44.48	0.6	113.4		0.8725						15.54
7	90		2660		9.169			1			1.413
8			184.8		9.169			0			
9			184.8		0.8725						
10	5		2510		0.8725			1			1.413
11	100				200				4.215		194.9
12	95										
13	18.33										186.5
14	23.33										186.5

15	18.33										167.2
16	23.33										167.2
17	12				101.3				4.192		156.7
18	7										
19	24		47.77			0.5	0.009				163.3
20	45		79.25	25.9	101.3		0.013				40.82
21	28.2		54.07				0.010				204.1
22	14		37.98			0.95	0.0094				204.1
23	15										240.1
24											
25	23.33										353.7
26	18.33										

Table 2: Values of different variables at different state points for the system given in Fig. 3

Point	T_i	Xi	hi	Bi	p_i	Ri	W_i	Q_i	c_i	v_i	m_i
1	34.46	0.55	83.21		0.8725					1.017	7.675
2		0.55	83.21		9.169						
3	79.2	0.55	175.5		9.169						7.675
4	90	0.6	214.1		9.169				1.957		7.035
5		0.6	113.4		9.169						
6	44.48	0.6	113.4		0.8725						7.035
7	90		2660		9.169			1			0.6396
8			184.8		9.169			0			
9			184.8		0.8725						
10	5		2510		0.8725			1			0.6396
11	100				200				4.215		88.26
12	95										
13	18.33										84.42
14	23.33										84.42
15	18.33										75.71
16	23.33										75.71

17	12				101.3				4.192		70.95
18	7										
19	24		47.77			0.5	0.009				163.3
20	45		79.25	25.9	101.3		0.013				40.82
21	28.2		54.07				0.010				204.1
22	14		37.98			0.95	0.009				204.1
23	15										108.7
24											
25	23.33										160.1
26	18.33										
27	15										

Figure (5) illustrates the variation of absorber, condenser, evaporator, and generator capacities with seawater temperature. It is observed that as the seawater temperature increases the capacity of each component increases. Also, the variation of the precooler capacity is inversely proportional to the seawater temperature as shown in Fig. (6). It is observed that the capacities of the components in either Fig. (5) or Fig. (6) are linearly varied with the seawater temperature.

The system coefficient of performance decreases with the increase of the generator temperature as illustrated in Fig. (7). by the help of Fig. (8) can be explained the state in which shows that the generator capacity is slightly increased with the increase of seawater temperature while the evaporator capacity does not change with the seawater temperature.

The mass of refrigerant (pure water) increases linearly with the increase of seawater temperature, as illustrated in Fig. (9) Because of the increase in the evaporator and condenser capacities. In addition, the mass of both weak and strong LiBr-H_2O solutions increases with the increase of seawater temperature as shown in Fig. (10). this may be due to the increase in both the absorber and generator capacities.

The variation of hot water mass flow rate required for the generator, cooling water for absorber and condenser as well as the chilled water with the seawater temperature is depicted in Fig. (11). From the figure, it is observed that the water mass flow rate of each cycle component increases with the increase of seawater temperature.

The percentage reduction of each component capacity due to the use of air precooling is illustrated in Fig. (12). the percentage reduction is 55% for seawater temperature of 15^{o}C and reaches 5% for seawater temperature of 27^{o}C.

Figure (13) shows that both the considered systems illustrated in Figs. (2) and (3) have the same value of COP and the COP value decreases with increasing of the generator temperature. The

variation of the number of transfer units, UA, for the refrigeration cycle components with the seawater temperature is demonstrated in Fig. (14), the figure shows as the seawater temperature increases the number of transfer units increases with higher values of the evaporator followed by generator, absorber, and condenser respectively. This may be due to the increase in the heat rate capacity of these components. The behavior is reversed for the precooler as shown in Fig. (15), as the seawater increases the number of transfer units of the precooler decreases.

Conclusions

From the findings, the following conclusions can be drawn:

1. The use of the air precooling process does not change the COP of the system but reduces the capacity of the components, which means the smaller sizes of the components.
2. The component size is reduced by 55% when the seawater temperature is 15^{o}C and by 5% when the seawater is 27^{o}C.
3. The decrease of COP of the systems with the increase of the generator temperature.
4. The increase in the seawater temperature leads to an increase in the number of transfer units of the refrigeration cycle and a decrease in the precooler number of transfer units.

REFERENCES,

[1] J. Aman, "Bubble-Pump-Driven Solar Absorption Air Conditioning for Residential Applications." University of Windsor (Canada), 2018. https://scholar.uwindsor.ca/etd

[2] "Statistical Review of World Energy 2021 | 70th edition." http://www.bp.com/statistical

[3] T. Babaei, H. Abdi, C. P. Lim, and S. Nahavandi, "A study and a directory of energy consumption data sets of buildings," Energy Build., vol. 94, pp. 91–99, 2015. http://dx.doi.org/10.1016/j.enbuild.2015.02.043

[4] G. Figueredo, M. Bourouis, A. Coronas (2008) "Thermodynamic modeling of a two-stage absorption chiller driven at two-temperature levels", Appl. Therm. Eng. 28, 211–7.

[5] S.C. Kaushik, A. Arora (2009) "Energy and exergy analysis of single effect and series flow double effect water–lithium bromide absorption refrigeration systems", Int J Refrig 32,1–12.

[6] Gomri Rabah (2010) "Investigation of the potential of application of single effect and multiple effect absorption cooling systems", Energy Convers Manage 51, 1629–36.

[7] M. Venegas, M.C. Rodríguez-Hidalgo, R. Salgado, A. Lecuona, P. Rodríguez, G. Gutiérrez (2010) "Experimental diagnosis of the influence of operational variables on the performance of a solar absorption cooling system", Appl Energy 88, 1447–54.

[8] C. Somers, A. Mortazavi, Y. Hwang, R. Radermacher, P. Rodgers, P. Al-Hashimi (2011) "Modeling water/lithium bromide absorption chillers in ASPEN Plus" Appl Energy 88, 4197–205.

[9] A.A.V. Ochoa, J.C.C. Dutra, J.R.G. Henríquez (2014) "Energy and exergy analysis of the performance of 10 TR lithium bromide/water absorption chiller", Revista Técnica de la Facultad de Ingeniería. Universidad del Zulia 37, 38–47.

[١٠] D.C. Wang, Y.J. Wang, J.P. Zhang, X.L. Tian, J.Y. Wu (2008) "Experimental study of adsorption chiller driven by variable heat source", Energy Convers Manage 49,1063–73.

[١١] M. Moya, J.C. Bruno, P. Eguia, E. Torres, I. Zamora, A. Coronas (2011) "Performance analysis of a trigeneration system based on a micro gas turbine and an air-cooled, indirect-fired, ammonia-water absorption chiller" Appl Energy 88, 4424–40.

[١٢] M. Izquierdo, J.D. Marcos, M.E. Palacios, A.G. González (2012) "Experimental evaluation of a low-power direct air-cooled double-effect LiBr–H_2O absorption prototype. Energy 37, 737–48.

[13] A.A.V. Ochoa, J.C.C. Dutra, J.R.G. Henríquez, C.A.C. dos Santos (2016) "Dynamic study of a single effect absorption chiller using the pair LiBr/H_2O", Energy Conversion and Management 108, 30–42.

[14] A.A.V. Ochoa, J.C.C. Dutra, J.R.G. Henríquez, C.A.C. dos Santos (2017) "The influence of the overall heat transfer coefficients in the dynamic behavior of a single effect absorption chiller using the pair LiBr/H_2O", Energy Conversion and Management 136, 270–282.

[15] Su Kyoung Lee, Jae Won Lee, Hoseong Lee, Jin Taek Chung, Yong Tae Kang (2019) "Optimal design of generators for H_2O/LiBr absorption chiller with multi-heat sources", Energy 167, 47–59

[16] T. Zhao, X. Chen, Q. Chen, (2020) "Heat current method-based modeling and optimization of the single effect lithium bromide absorption chiller", Applied Thermal Engineering 175, 115345.

[17] D. Surroop and A. Abhishekanand, "Technical and Economic Assessment of Seawater Air Conditioning in Hotels," Int. J. Chem. Eng. Appl., vol. 4, no. 6, pp. 382–387, 2013. DOI: 10.7763/IJCEA.2013.V4.330

[18] Y. Song, Y. Akashi, J. Yee (2007) "Effects of utilizing seawater as a cooling source system in a commercial complex", Energy and Buildings 39, 1080–1087, doi:10.1016/j.enbuild.2006.11.011

[19] A. F. Elsafty and L. A. Saeid, "Seawater air conditioning [SWAC]: A cost-effective alternative," Int. J. Eng., vol. 3, no. 3, pp. 346–358, 2009.

[20] M. Delphi and S. M. Mosaddad, "Formation of summer thermocline in the Persian Gulf," Int. J. Environ. Sci. Dev., vol. 1, no. 5, pp. 429–431, 2010.

[21] G.A. Florides, S.A. Kalogirou, S.A. Tassou, L.C. Wrobel, (2003) "Design and construction of a LiBr–water absorption machine", Energy Conversion and Management 44 2483–250.

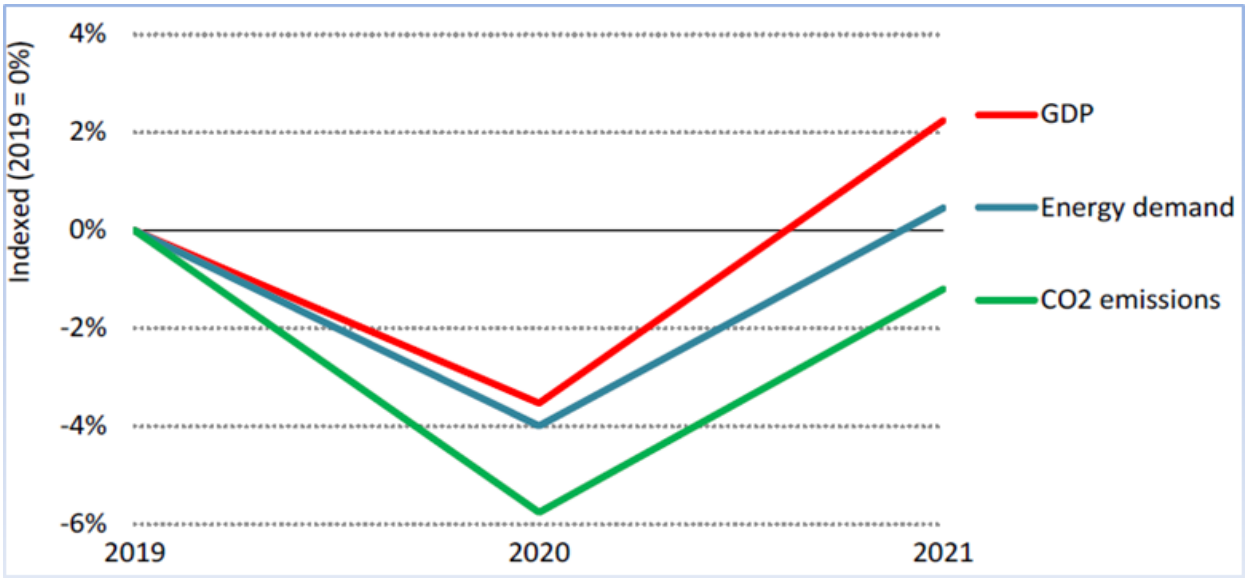

Fig.1: Global actual and predicted energy demand.

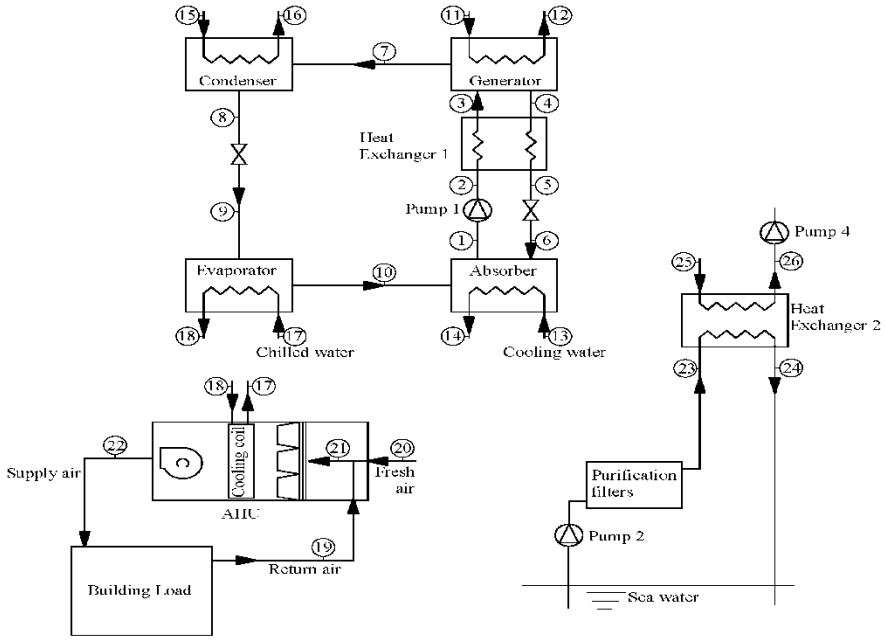

Fig. 2: Air- conditioning single effect LiBr-H_2O absorption system using seawater for cooling the condenser and absorber and without precooling

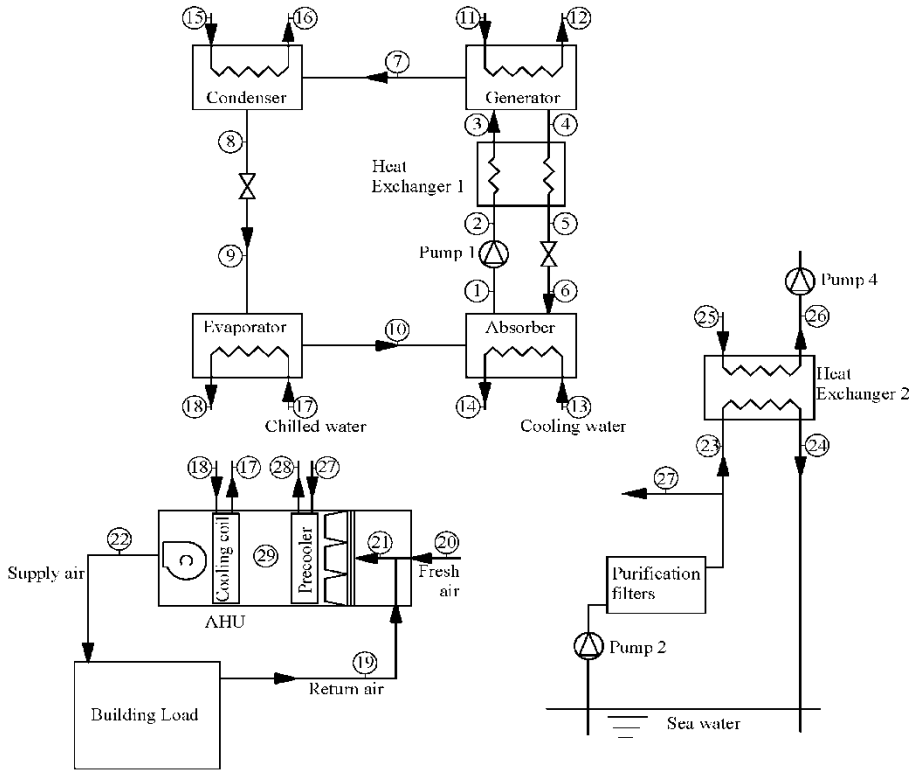

Fig. 3: Air- conditioning single effect LiBr-H_2O absorption system using seawater for cooling the condenser and absorber with air precooling

Fig.4: precooling process on psychometric chart

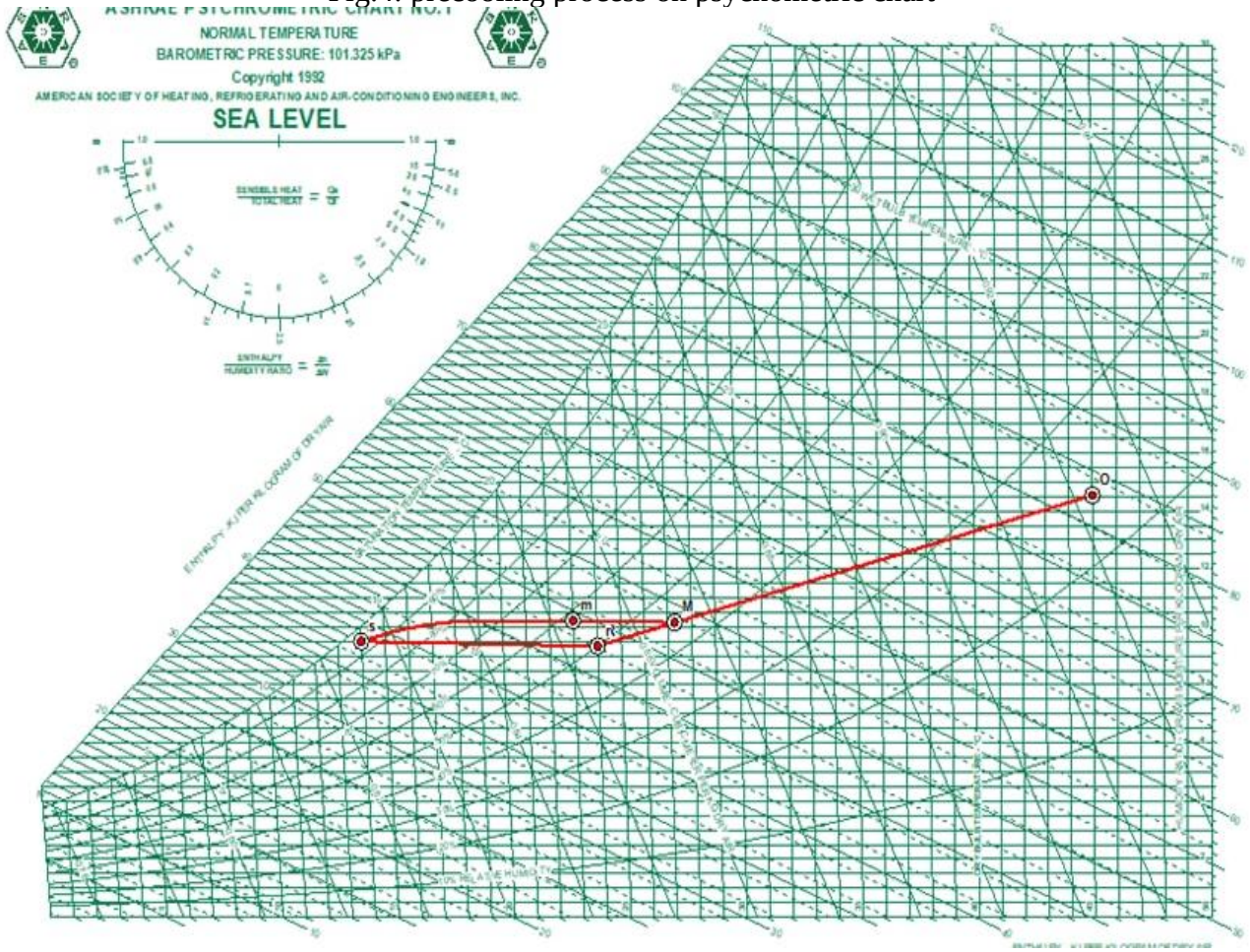

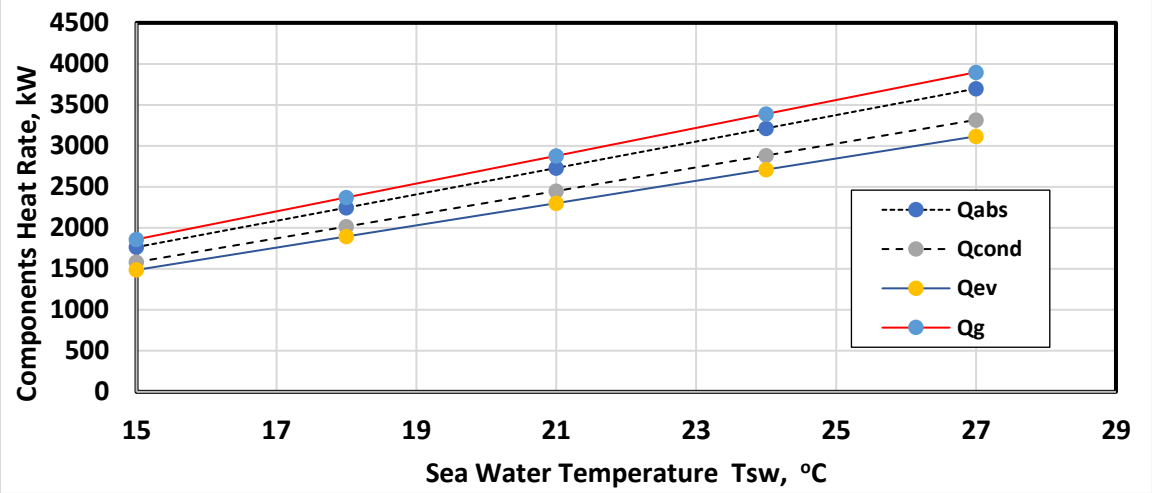

Fig. (5) Variation of heat rate of refrigeration cycle's components with seawater temperature

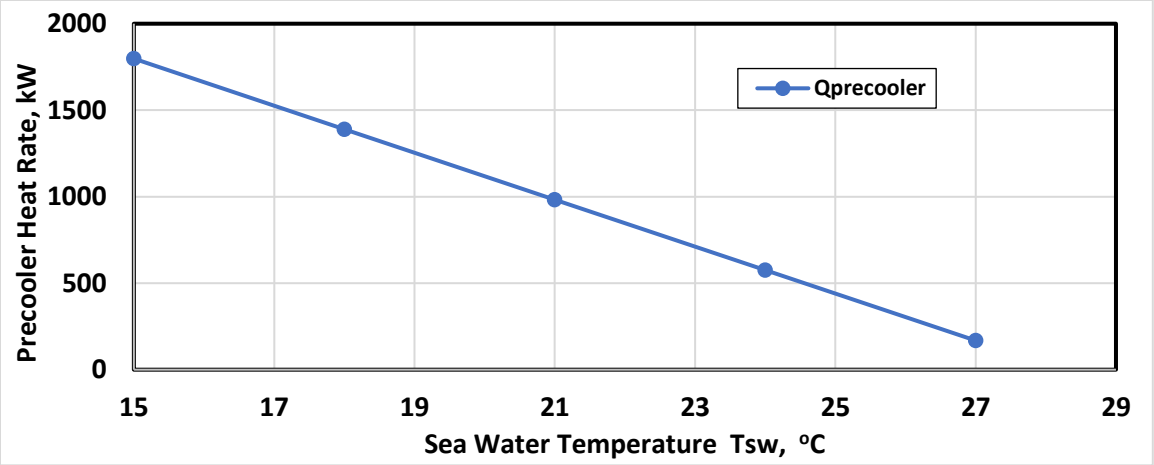

Fig. (6) Variation of Precooler heat rate with seawater temperature

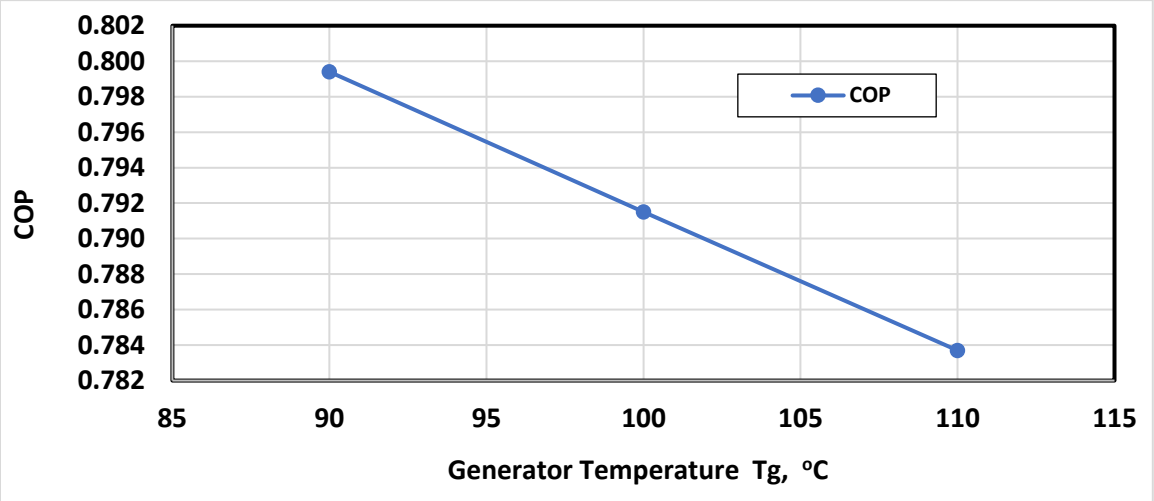

Fig. (7) Variation of COP with the generator temperature

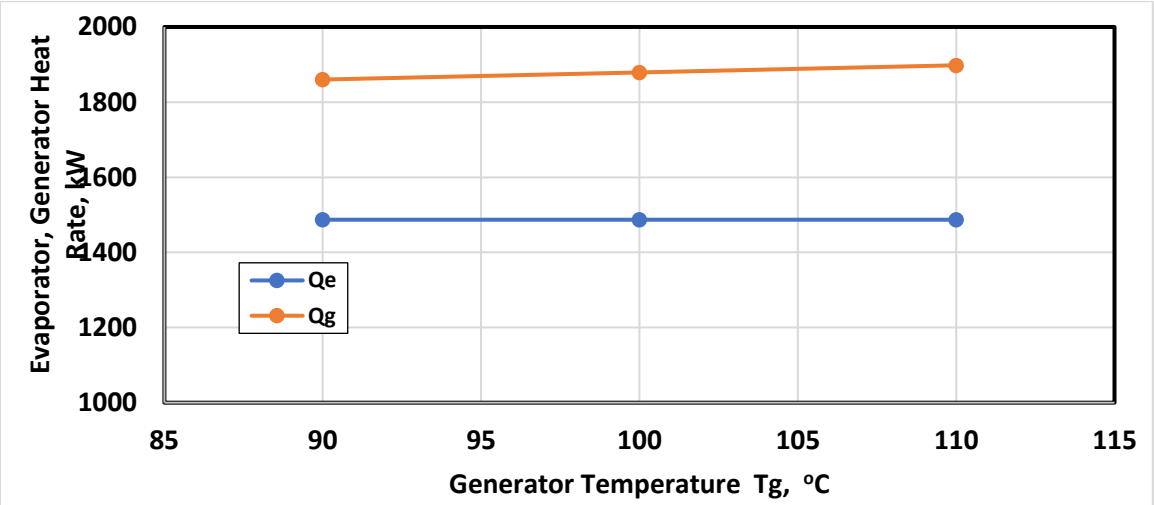

Fig. (8) Variation of evaporator and generator heat rate with the generator temperature

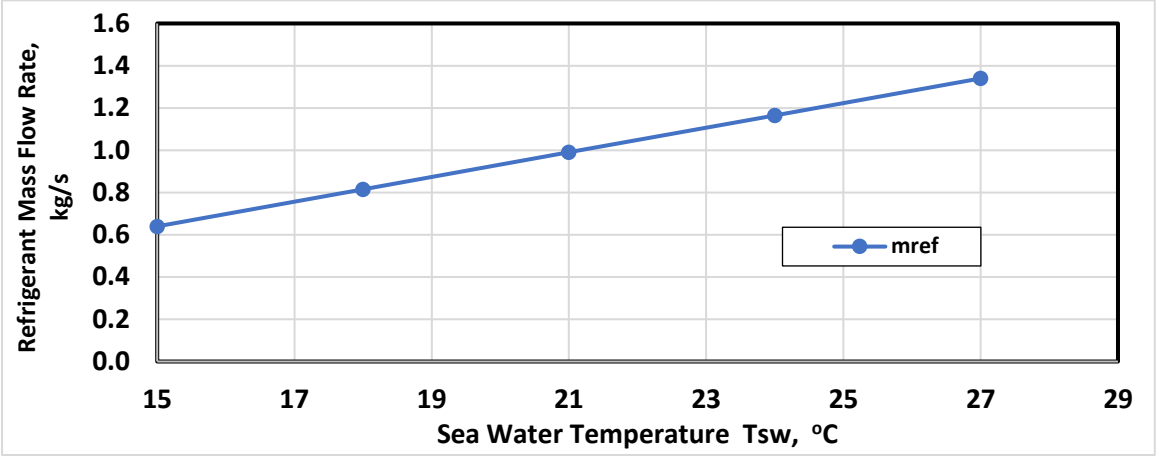

Fig. (9) Variation of evaporator and generator heat rate with the generator temperature

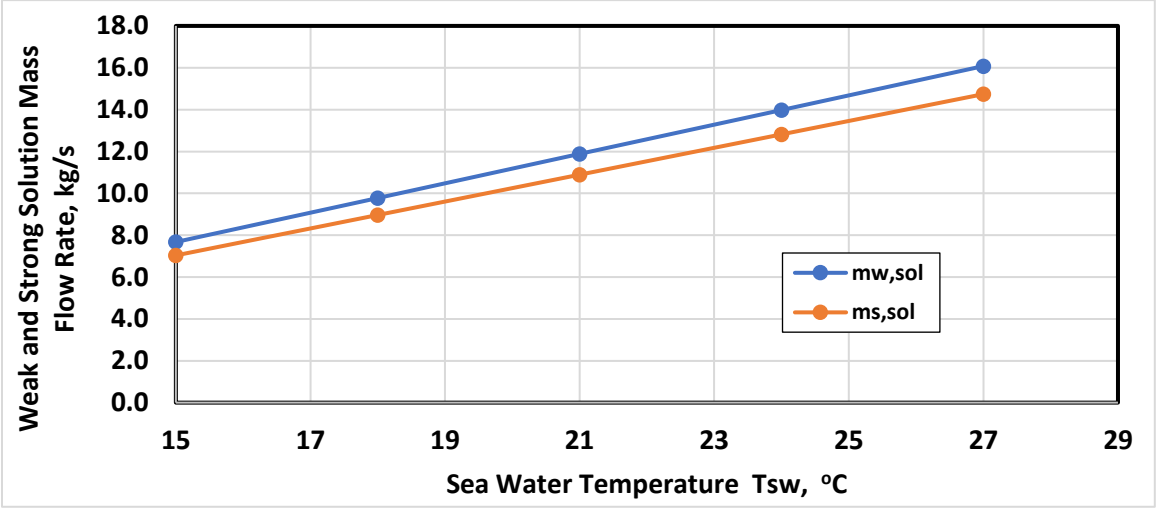

Fig. (10) Variation of weak and strong solution mass flow rate with the seawater temperature

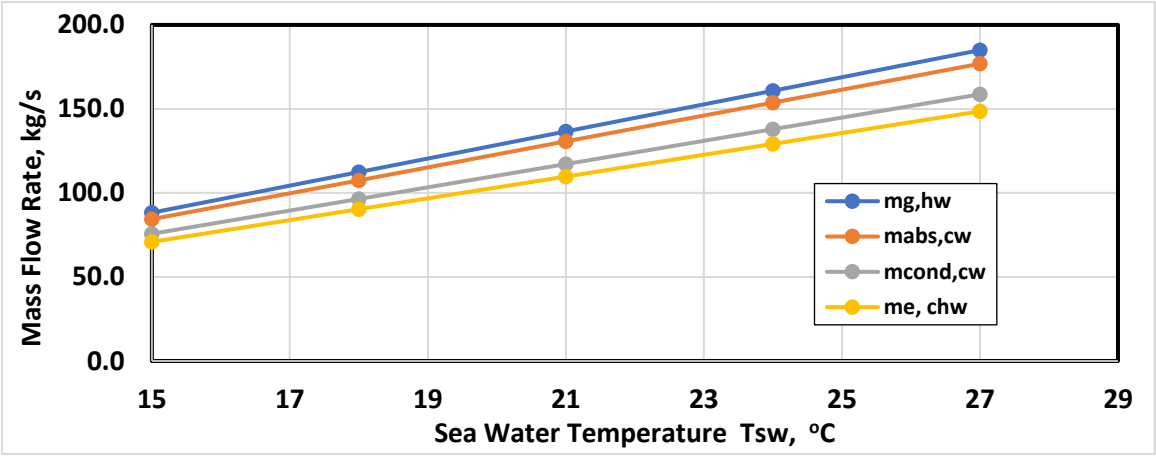

Fig. (11) Variation of water mass flow rate of generator, absorber, condenser, and evaporator mass flow rate with the seawater temperature

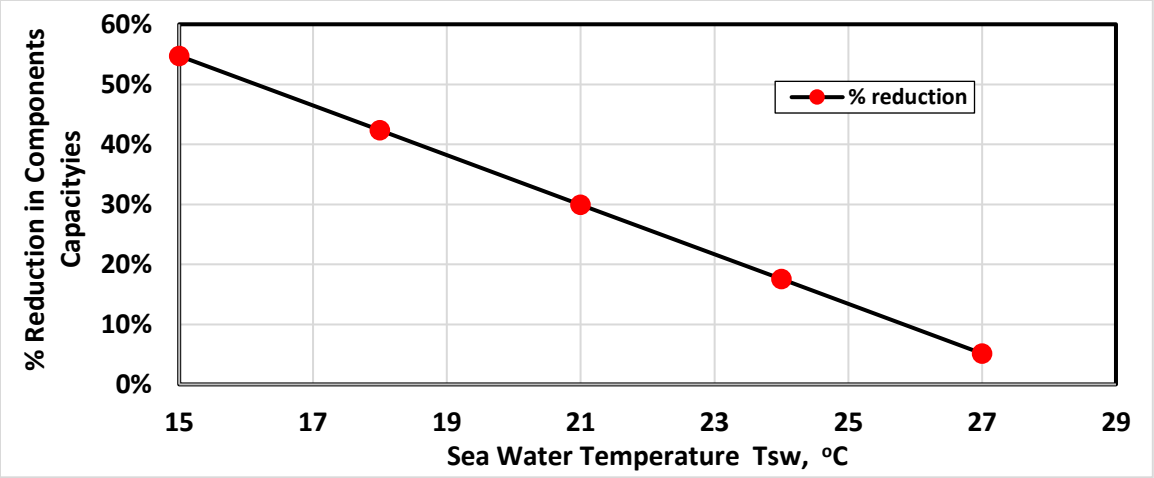

Fig. (12) Variation of percentage reduction in components capacities with the seawater temperature

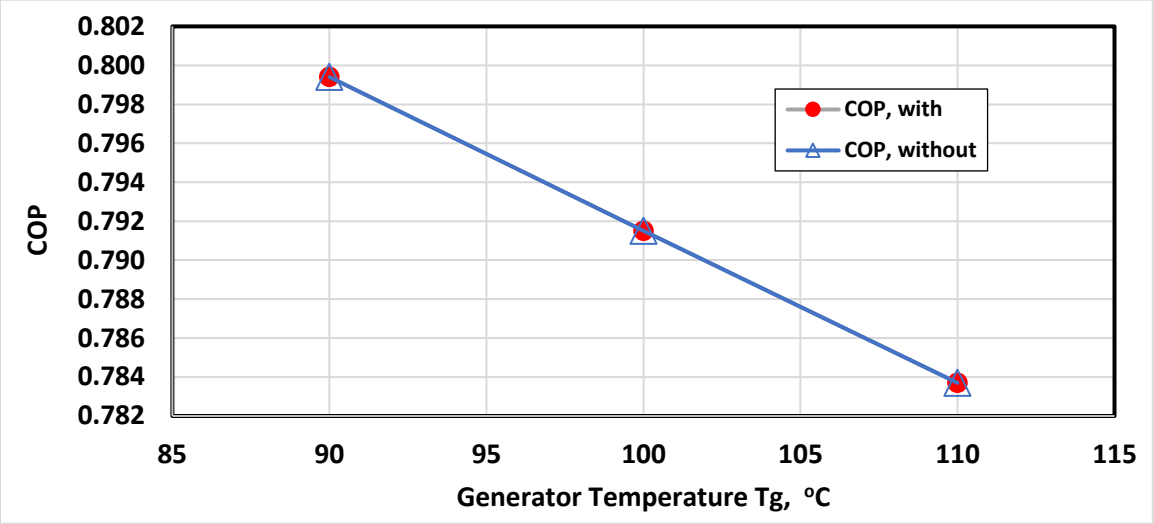

Fig. (13) Variation of COP with the seawater temperature with and without seawater air precooling

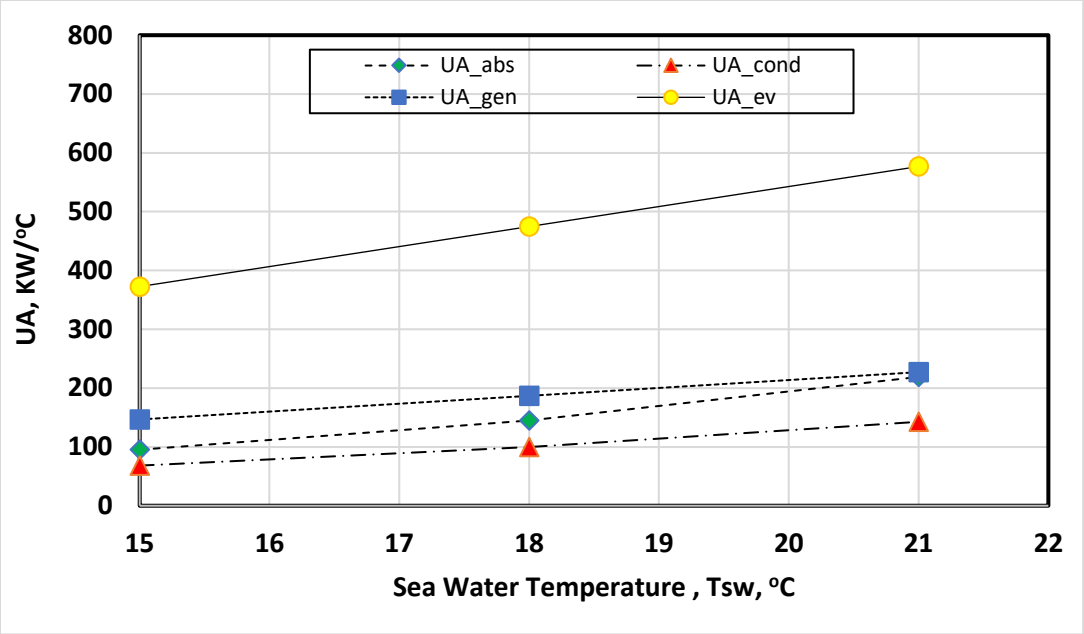

Fig. (14) Variation of refrigeration cycle's components (UA) with the inlet seawater temperature

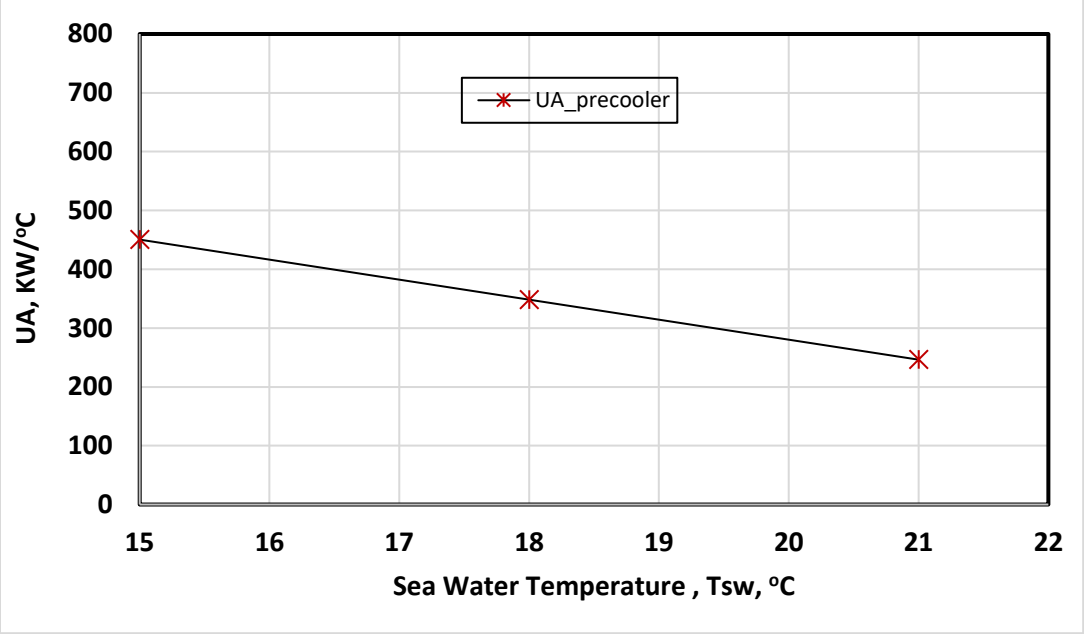

Fig. (15) Variation of precooler (UA) with the inlet seawater temperature